Green Chemistry

PAPER

View Article Online
View Journal

Cite this: DOI: 10.1039/c4gc02333a

A non-nitric acid method of adipic acid synthesis: organic solvent- and promoter-free oxidation of cyclohexanone with oxygen over hollow-structured Mn/TS-1 catalysts†

Guoqiang Zou, Wenzhou Zhong,* Liqiu Mao, Qiong Xu, Jiafu Xiao, Dulin Yin,* Zisheng Xiao, Steven Robert Kirk and Tao Shu

Received 26th November 2014,
Accepted 21st January 2015

DOI: 10.1039/c4gc02333a

www.rsc.org/greenchem

A novel hollow-structured Mn/TS-1 catalyst has been reported as a non-nitric acid route for adipic acid production from oxidative cleavage of cyclohexanone. The method generates adipic acid in high yields with molecular oxygen under organic solvent- and promoter-free conditions. The hollow nature of the catalyst with large intra-particle voids facilitates the diffusion of bulky molecules to the internal catalytic site and increases the catalyst activity. The advantage of this catalyst is its reusability with almost consistent reactivity, thereby making it viable for industrial applications.

1. Introduction

The development of a new and efficient methodology for the production of bulk chemicals, in particular one that takes account of effects on the environment, is becoming more and more important in industrial chemistry worldwide.[1] Adipic acid (AA) is an important raw chemical for the production of nylon-6,6, fibers, plasticizers, food additives, *etc.*[2,3] The world production capacity of AA was around 3 million metric tons in 2006 and the demand for it has increased every year in the last decade.[4] The traditional industrial process utilizes the nitric acid oxidation of cyclohexanone and/or cyclohexanol (KA oil) which are derived from benzene (Fig. 1).[5,6] The main drawback of this processing is the emission of large amounts of the strong greenhouse gas (N_2O), an inevitable waste causing global warming and ozone depletion as well as acid rain and smog.[7,8]

Many efforts have been made to improve or even get rid of this conventional process. Syntheses starting from cyclohexanone, cyclohexanol, cyclohexene and cyclohexane were actually widely developed.[9–12] Chavan *et al.* have used a Co/Mn cluster complex as a catalyst to convert cyclohexanone to AA in acetic acid medium with a selectivity of 86%.[9] Sato *et al.* oxidized cyclohexanol with 30% H_2O_2 over H_2WO_4, which achieved about 78% yield.[10] Holmberg and coworkers oxidized cyclohexene with 30% H_2O_2 to AA over WO_3-containing mesoporous oxide.[11] Recently, Thomas *et al.* have reported a single-step, liquid-phase, aerial oxidation of cyclohexane to AA (selectivity of AA = 32.2% at cyclohexane conversions of 19.8% and 1.5 MPa).[12] While some positive outcomes were obtained, the price of the oxidants such as H_2O_2 and *tert*-butylhydroperoxide, the drastic reaction conditions, additional organic solvents, and the low yields of AA restricted the industrial application of these new developments. Thus, an environmentally friendly, yet practical route to AA from cyclohexanone using cheaper oxidants such as O_2 without any solvents is highly desirable. The challenge, however, is the development of an efficient and stable catalyst that would make this new route competitive compared with the nitric acid route.

Titanosilicate molecular sieves TS-1, with MFI cages connected by 10-ring pore openings, have been known for their remarkable selective oxidation activity for organic molecules in the chemical industry.[13] The diffusion and transport of large molecules within such microporous channels would, however,

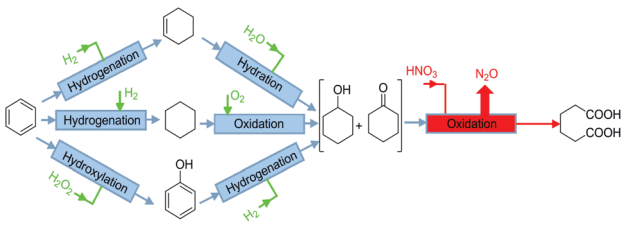

Fig. 1 Current industrial processes.

National & Local United Engineering Laboratory for New Petrochemical Materials & Fine Utilization of Resources, Hunan Normal University, Changsha 410081, P. R. China. E-mail: zwenz79@163.com, dulinyin@126.com; Tel: +86-731-88872576; Fax: +86-731-88872531

†Electronic supplementary information (ESI) available. See DOI: 10.1039/c4gc02333a

be greatly limited by the small pore openings, resulting in low catalytic activity in the oxidation of bulky substrates. In contrast, large-pore Ti-Beta and Ti-MCM were anticipated to solve the diffusion and transport problems encountered in the oxidation of bulky molecules, but they have not been able to substitute for traditional TS-1 as catalysts in industrial chemistry mainly due to the presence of Brønsted acid sites associated with the aluminum framework or their low hydrothermal stability resulting from the absence of a zeolite-like crystalline framework.[14–16] Therefore, a novel large-pore structure (or one with large intra-particle voids) which does not have the aforementioned disadvantages is urgently desired. In particular, large intra-particle voids in a structure can greatly favor the mass transport ability of a guest molecule to internal catalytic sites.[17] In the past few decades, various types of Ti-containing zeolites have been prepared and some encouraging results have been reported by the 'destructive' and the 'constructive' synthesis methods.[18–21] Among the Ti-containing zeolites, a kind of hollow-structured TS-1 catalyst (HTS) has received much attention in the selective oxidation of bulky molecules such as cyclohexane and shown to be more active than TS-1 with H_2O_2 as the oxidant.[21] H_2O_2 is, however, an expensive oxidant, and its extensive application will be seriously limited. This arouses our research interest in using other cheap oxidants such as molecular oxygen to carry out the oxidation of bulky molecules.

In a previous paper, we reported on the catalytic behaviour of Mn-doped titanosilicate with a hollow structure in the aerobic oxidation of cyclohexane to AA conducted in a free-solvent.[22] It was found that the hollow structure and Ti sites in the internal surface are more adapted for the production of bulky AA compared with cyclohexanol or cyclohexanone. However, the cyclohexane conversion and AA yield achieved were relatively low in industrial chemistry. In this paper, we report the aerial oxidation of cyclohexanone to AA using this hollow-structured TS-1 catalyst. To our knowledge this is a novel non-HNO_3, aerial oxidation route for the preparation of AA from cyclohexanone, without the addition of an additional solvent or initiator, wherein the yields of AA are comparable to those obtained in current, commercial practice. In addition, this solvent-free/dioxygen system can suppress the leaching of active metal ions during heterogeneous reaction. This method would provide new possibilities for applying titanosilicates in the petrochemical and fine chemical industries.

2. Experimental

2.1. Synthesis of the catalytic materials

TS-1 was synthesized hydrothermally using tetraethyl orthosilicate (TEOS) and titanium butoxide (TBOT) as the sources of Si and Ti, respectively, whereas alkali-free tetrapropyl ammonium hydroxide (TPAOH) and anhydrous isopropanol were used as the template and mobilizing agent for the formation of micropores, respectively. The starting gel was formed using the following molar compositions: $SiO_2 : 0.4TPAOPH : 0.01TiO_2 : 40H_2O$ and was transferred to a Teflon-lined stainless steel autoclave. Crystallization was carried out by placing the sealed autoclave in an air oven maintained at 443 K for 3 days. The product obtained was filtered, washed with distilled water, dried at 393 K and finally calcined at 793 K for 10 h. The HTS was synthesized according to a literature method.[23] The previously calcined TS-1 was treated with H_2SO_4 solution with a weight ratio of the TS-1 : H_2SO_4 : water = 10 : 1.0 : 140 for 3 h at room temperature. The acid-treated TS-1 was dispersed in TPAOPH solution in a weight ratio of 10 TS-1 : 1.5 TPAOPH : 125 H_2O and was recrystallized at 413 K for 3 days under static conditions. The solid product was filtered, washed, dried and finally calcined at 793 K for 10 h.

The catalyst Mn-modified HTS was prepared by the incipient wetness impregnation of HTS with an EtOH and water (1 : 1) solution of manganese acetate to give 5 wt% of manganese in the final product. The volume of the solution used was sufficient to completely wet the HTS sample. The impregnated sample was slowly allowed to evaporate at 373 K till dryness, followed by calcination at 773 K in air for 3 h (with a heating rate of 5 °C min^{-1}). The investigated samples were referred to as *x*Mn-HTS, where *x* denotes the metal wt%.

2.2. Catalyst characterization

X-ray powder diffraction patterns (XRD) were recorded on a Bruker Advanced D8 diffractometer using CuKα radiation (λ = 1.542 Å). Size and particle morphology of the samples were determined using scans obtained using a Hitachi S-4800 microscope, while the TEM images were taken by using a JEOL-JEM-2100 microscope. The textural properties of the samples were measured by N_2 adsorption at 77.4 K using a Tristar 3000 sorptometer. Prior to the tests, the samples were outgassed at 473 K under a reduced pressure of 10^{-5} Torr for 3 h. The surface area was determined by the Brunauer–Emmett–Teller (BET) equation, while the total pore volume was measured at p/p_0 = 0.99. The pore size distributions were determined from the adsorption branch of the isotherms using the BJH method. The UV-visible diffuse reflectance spectra of the samples were recorded from 190 to 500 nm with a Varian-Cary 5000 spectrometer using $BaSO_4$ as a reference. X-ray Photoelectron Spectra (XPS) of samples were recorded with an Imaging Photoelectron Spectrometer (Axis Ultra, Kratos Analytical Ltd) using Al Kα radiation (1486.7 eV). The energy was calibrated with a C 1s peak (BE = 284.8 eV). Fit XPS software was used for curve fitting. Pyridine-adsorbed FT-IR spectra were recorded using a PerkinElmer Spectrum 100 spectrometer. The samples were subjected to a conditioning treatment *in situ* in advance, which involved outgassing at 473 K for 2 h (residual pressure at 1.33×10^{-2} Pa) and then cooling down to room temperature and equilibrating with pyridine for 15 min. After heating at 423 K for 0.5 h, recordings of the FT-IR spectra were collected.

2.3. Cyclohexanone oxidation reaction

The catalytic oxidation of cyclohexanone was carried out in a Teflon-lined stainless steel autoclave of 100 cm^3 capacity,

equipped with a magnetic stirrer. In a typical experiment, cyclohexanone (40 g) was mixed with 0.4 g of the catalyst and then heated to 363 K. Oxygen was then charged into the reactor to the desired pressure and the reaction was started by adjusting the stirrer speed to 450 rpm. After the reaction, the mixture was cooled down, dissolved in ethanol and filtered. The reaction mixtures were analyzed by using an Agilent 1100 series high-performance liquid chromatography instrument equipped with a UV detector (Agilent G1365B MWB), using a column of Zorbax Eclipse XDB C18 (150 mm × 4.6 mm i.d.). The compounds of the reaction mixture were quantified by HPLC using heptane diacid as the internal standard and identified by HPLC-MS. The quantitative analyses of unreacted cyclohexanone were carried out by gas chromatography using chlorobenzene as the internal standard. Mass balances were verified.

3. Results and discussion

3.1. Structural analysis

The XRD patterns of samples shown in Fig. S1 in the ESI† indicate that all the prepared HTS and 5% Mn-HTS samples retain the MFI-type phase structure of zeolite TS-1 and no diffraction peaks corresponding to crystalline MnO_x clusters could be detected.[24] It is, therefore, believed that the manganese species have homogeneously dispersed on the surface of the crystals. The crystallinity and morphology of HTS synthesized by a dissolution–recrystallization process were investigated by TEM. The particles of HTS and 5% Mn-HTS showed large intra-particle voids with an average particle size of 150–250 nm, and the large voids were located exclusively in the inner part of the crystals and never communicating directly with the surface (see Fig. 2A and C). This kind of hollow nature is essential to decrease pore diffusion limitations and facilitate bulky molecular transport to catalytic sites and increase the activity of the catalyst, which is similarly observed in earlier reports.[25] The TEM results in Fig. 2C and D confirmed that manganese species were dispersed onto the hollow

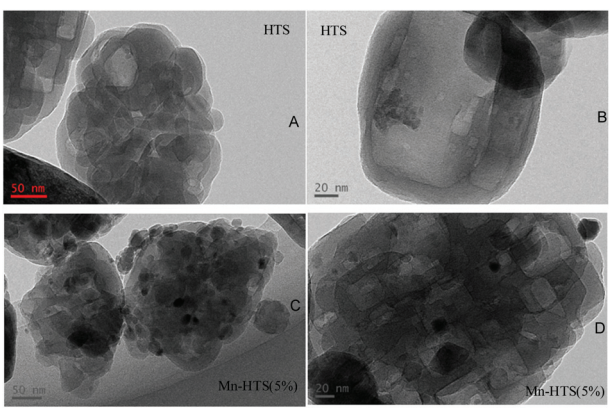

Fig. 2 TEM images of the parent HTS (A and B) and 5% Mn-HTS samples (C and D).

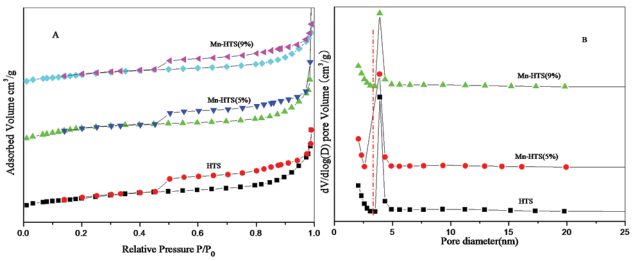

Fig. 3 (A) N_2 adsorption–desorption isotherms and (B) pore diameter distribution of the parent HTS and the *x*Mn-HTS samples.

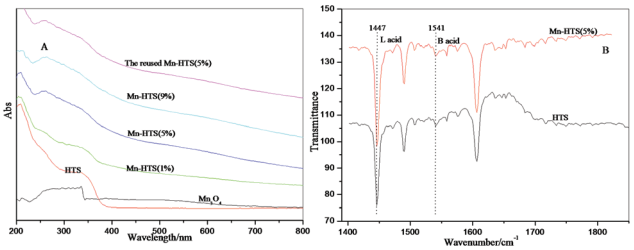

Fig. 4 (A) UV-Vis and (B) pyridine-adsorbed FT-IR spectra of the parent HTS and the *x*Mn-HTS samples.

structured zeolite surface. Furthermore, a crystalline material containing no amorphous phase could also be clearly found, indicating their high hydrothermal stability during the reaction. N_2 adsorption/desorption isotherms and pore size distributions for samples of the hollow-structured zeolite HTS and the prepared Mn-HTS are shown in Fig. 3. The presence of intra-crystalline voids accessible only *via* entrances smaller than 4 nm is evident from abrupt closure at $p/p_0 = 0.42$ on the desorption branch and differ from those of normal TS-1, as evidenced by TEM images.[23] After loading with Mn species, the samples showed similar N_2 sorption isotherms with a H_2 hysteresis to that of matrix HTS, indicating the presence of a similar structure with intra-crystalline voids. The Ti coordination states of HTS after calcination were studied by UV-visible spectroscopy (Fig. 4A). One band centered at 220 nm could be observed for HTS, which can be attributed to the charge transfer from O^{2-} to Ti^{4+} and is characteristic of tetrahedrally coordinated Ti highly dispersed in hollow crystals, as they are in the original TS-1 zeolite.[26] Another band centered at 330 nm also appeared, however, most likely reflecting the presence of ex-framework Ti species (*e.g.*, octahedral Ti sites).[27] The big difference from the original TS-1 strongly supports the conclusion that the partial dissolution and recrystallization of the zeolite can modify the repartition of Ti species and enrich the surface of hollow crystals with the catalytic species.[23] Compared with the reference HTS, the prepared Mn-HTS displayed an absorption band at 310 nm (O^{2-} to Mn^{3+} electron transition) which might be somewhat hampered by overlap of the second assignments in the matrix HTS.[28] The change of the absorption band at 310 nm, however, clearly supports the assertion that manganese species are present on the surface of the catalyst.

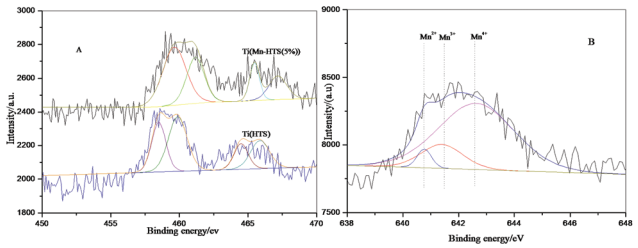

Fig. 5 (A) Ti(2p) core level XPS, (B) Mn(2p) core level XPS of the parent HTS and the *x*Mn-HTS samples.

The X-ray transmission spectroscopy (XPS) results in Fig. 5A showed that the sample of HTS possessed binding energy levels of Ti $2p^{3/2}$ and Ti $2p^{1/2}$ at around 459 eV and 464 eV, respectively. Interestingly, the curves for Mn-HTS shifted to larger binding energy, indicating that the Ti–O bonding strength was changed by the introduction of manganese ions.[29] For comparison, the Gaussian values were used in the curve resolution of the Ti $2p^{3/2}$ peaks. Two spectra were observed: the first peak at *ca.* 458.5 eV was assigned to the octahedrally coordinated Ti^{4+} ion and the second peak at *ca.* 460.0 eV was assigned to Ti^{4+} in the tetrahedral coordination within the silica framework. The relative area ratio of the peak at 460.0 eV assigned to tetrahedral Ti species, however, decreased with the loading of Mn, suggesting a change in the coordination number of titanium by the formation of a Ti–O–Mn bond.[30] In addition, the Mn $2p^{3/2}$ signal can be deconvoluted to distinguish the states of $Mn^{\delta+}$ and the results are recorded in Fig. 5B. The binding energies (BE) of Mn $2p^{3/2}$ in the intervals 639.9–640.8 eV, 640.5–642.3 eV and 642.5–643.2 eV can be attributed to the presence of Mn^{2+}, Mn^{3+} and Mn^{4+} ions on the surface of Mn-HTS, respectively.[31]

The surface acidities of samples were characterized by the pyridine-adsorbed FT-IR spectra of HTS and 5% Mn-HTS (see Fig. 4B). The two bands at 1450 cm^{-1} and 1540 cm^{-1} corresponded to Lewis acid sites and Brønsted acid sites, respectively.[32] It is apparent that both the catalysts possess many more Lewis acid sites than Brønsted acid sites. The introduction of Mn species leads to an increase in the number of Lewis acid sites, possibly because a few percent of the Ti species are coordinated by high valence Mn species.

3.2 Activities of the catalysts

Table 1 shows the activities of the different metal-modified HTS catalysts in the selective oxidation of cyclohexanone in the liquid phase using oxygen as an oxidant. The hollow-structured Mn-HTS catalyst showed 68.4% cyclohexanone conversion with 93.1% AA selectivity (Table 1, entry 5); the main by-product was glutaric acid (GA). Compared with the Mn-HTS catalyst, some other metal-modified HTS catalysts such as Co-HTS, Fe-HTS, Cr-HTS, Cu-HTS, or V-HTS (Table 1, entries 6–10) were much less effective for the catalytic oxidation of cyclohexanone into AA. It is clear that the oxidation activity is dependent on the nature of the metal used.[33] In addition, the lower activity observed in the reaction using Mn-TS as the catalyst in comparison with Mn-HTS is presumably due to the solid structure of the Mn-TS catalyst (Table 1, entry 11). According to the TEM and N_2 sorption isotherms results that show large intra-crystalline voids of Mn-HTS (see Fig. 2 and 3), we may capitalize here on 'product shape-selectivity'. Considering the large intra-crystalline voids of Mn-HTS, substrate conversion likely occurs inside the intra-crystalline voids of the Mn-HTS catalyst. Only those products with appropriate molecular dimensions may diffuse easily out of the intra-crystalline voids *via* the pore, whereas larger ones formed in the course of the reaction are trapped inside on account of their significantly retarded diffusion. Qualitatively, the diameter of cyclohexanone is 0.51 nm (the distance between oxygen and the most distant hydrogen is 0.50 nm; the van der Waals radius of hydrogen is 0.10 nm) and that of the products cyclohexyl hydroperoxide (CHHP) and AA should be 0.69 and 1.0 nm, respectively; the average pore diameter of HTS-1 is 0.55 nm. We therefore envisage that molecular cyclohexanone can enter the intra-crystalline voids of the Mn-HTS catalyst *via* the pore. Reaction intermediates (cyclohexyl hydroperoxide, ketonyl radical complex) formed within the intra-crystalline voids, however, will be held in the vicinity of the active centres, until oxidation proceeds further to yield the more mobile and desired linear product AA.

With respect to active centres, detailed comparisons (Table 1, entries 2–4) with silicate-1 and TS-1 leave no doubt that the active sites in our highly active catalyst are enriched Ti species on the surface of intra-crystalline voids. One of the key features of our approach to the design of the necessary cata-

Table 1 Cyclohexanone oxidation with O_2 over HTS catalysts[a]

			Selectivity[c] (%)			
Entry	Catalyst	Conversion[b] (%)	AA	GA	SA	Others
1	Blank	1.8	93.9	6.1	—	—
2	Silicon-1	1.9	93.4	6.3	—	0.3
3	TS	6.7	94.6	5.4	—	—
4	HTS	27.3	95.5	4.5	—	—
5	Mn-HTS	68.4	93.1	6.9	—	—
6	Co-HTS	22.4	78.6	11.6	4.7	5.1
7	Fe-HTS	36.9	78.8	13.2	4.1	3.9
8	Cr-HTS	28.4	67.4	29.0	2.5	1.1
9	Cu-HTS	30.6	71.6	28.4	—	—
10	V-HTS	25.0	65.1	21.2	6.4	7.3
11	Mn-TS	11.2	92.8	4.3	2.9	—
12[d]	Mn-HTS	2.4	95.4	4.6	—	—
13[e]	Mn-HTS	53.6	85.2	12.3	2.5	—
14[f]	Mn-HTS	61.4	85.5	11.6	2.4	0.5
15[g]	Mn-HTS	57.9	87.8	10.4	1.8	—
16[h]	Mn-HTS	—	—	—	—	—

[a] Reaction conditions: cyclohexanone (40 g), catalyst (0.4 g, 5 wt% of metal), O_2 (0.6 MPa), 363 K, 9 h. [b] Cyclohexanone conversion based on cyclohexanone consumed. [c] Product selectivity = content of this product/the cyclohexanone consumed, AA: adipic acid; GA: glutarate acid; SA: succinate acid; others: probably CO_2 and CO. [d] Mn-HTS was treated with trimethylamine. [e] Mn-HTS was treated with triphenylamine. [f] Addition of acetic acid (0.2 g), 6 h. [g] Addition of adipic acid (0.2 g), 6 h. [h] Addition of 2,6-di-*tert*-butyl-*p*-cresol (5 mol% cyclohexanone), 20 h.

lysts is to implant transition metal Mn ions in high oxidation states onto the surface of the crystals by calcination. The resulting catalyst, with a modified active site, exhibits an activity for the oxidation of cyclohexanone that surpasses that of the original catalyst (Table 1, entries 4 and 5). There is clearly a favourable electronic influence in proceeding from a $(SiO)_3Ti$–OH to a $(SiO)_2(MnO)Ti$–OH, as demonstrated by DR-UV and XPS (see Fig. 4A and 5A). Furthermore, the location of the active Ti sites in Mn-HTS was studied by using position-selective poisoning reagents. We selected two molecular probes: (1) tripropylamine (TPA), which is expected to enter the intra-crystalline voids of the catalyst and consequently poison the Ti sites, and (2) the bulky triphenylamine (TPhA), which is too large to enter the intra-crystalline voids of the catalyst *via* entrances and thus should selectively poison the active Ti sites located at the surface of intra-crystalline voids. In the case of TPA, after the reaction, the cyclohexanone conversion showed a dramatic yet comparable decrease (Table 1, entries 12 and 13), suggesting that most of the Ti sites participating in the oxidation of cyclohexanone with oxygen are located within intra-crystalline voids at the surface of the HTS-1 particles.

3.3 Effect of various parameters

In order to further understand the product distribution in the cyclohexanone oxidation, we studied the effect of reaction parameters. The catalyst shows a low activity with 100% AA selectivity at 353 K but with increasing temperature the conversion of cyclohexanone increased. At 363 K, we found that the formation of AA was optimum. At a higher temperature (393 K), the yield of adipic acid dropped significantly (Fig. 6A). Most probably the product AA could be continuously oxidized into by-products under the elevated temperatures. Fig. 6B shows the effect of reaction time on both cyclohexanone conversion and adipic acid selectivity. It is well observed that with increasing time, initially the conversion of cyclohexanone (till 3 h) increases slightly, but after 3 h the conversion of cyclohexanone increases very rapidly. In the meantime, it was also found that the AA selectivity decreased slightly. A possible explanation for this phenomenon is a radical-type autoxidation process. In order to find out the reaction intermediates, we took aliquots of the sample at regular intervals and analysed them by iodometric titration. No hydroperoxide was detected, which indicates that these possible reaction intermediates are quickly transformed into more stable diacids.[34] The amount of Mn loading was found to be very important, since lower Mn loading decreased the reaction rate without affecting the AA selectivity significantly (Fig. 6C). We have also explored the effect of the catalyst-to-cyclohexanone mass ratio on catalytic behaviour (Fig. 6D). There was an almost proportional effect of the catalyst amount on cyclohexanone conversion (with a catalyst-to-cyclohexanone mass ratio as low as 1×10^{-2}), whereas the selectivity to the products was not affected much by the conversion. After the initial rapid increase, a further addition of a catalyst led to a negative effect on the conversion and AA selectivity, which might be due to the well-known chain-termination effect.[35] Moreover, it cannot be excluded that a redox-type mechanism may prevail over autoxidation under conditions of a high catalyst-to-cyclohexanone mass ratio based on the distribution of products.[34] These results indicate a direct participation of the catalyst in the rate-determining step of the process, and suggest that the Mn-HTS has a catalytic effect on the process rate. The conversion of cyclohexanone and AA selectivity has a complicated dependence on the molecular oxygen pressure as shown in Fig. S2 in the ESI.† The maximum yield of AA was observed at 0.6 MPa of molecular oxygen pressure. At lower or higher pressures, selectivity of AA decreased significantly.

3.4 Reuse of the Mn-HTS catalyst

From the context of a 'green' approach, the catalytic oxidation of cyclohexanone was performed with a reused Mn-HTS catalyst under the same reaction conditions. The catalytic activity of the recovered catalyst after 15 consecutive experiments did not lead to any significant decline in its efficiency in terms of conversion and selectivity (Fig. 7A). After completion of the reaction, the solid catalyst was removed from the reaction mixture by filtration during the hot conditions and the oxidation was allowed to proceed with the mother liquor (filtrate) under the same conditions. The conversion did continue to increase, albeit at a much lower rate after the removal of the catalyst (Fig. 7B). The persistence of a low activity could be attributed to the thermal autoxidation, initiated by the oxygenated products, present in the mother liquor.[36] The leaching test was carried out for Ti and Mn by ICP-AES analysis using the filtrate and it was found that no Ti or Mn ions were present in the filtrate. We also observed that the amount of Ti and Mn present in the reused catalyst after 15 cycles of reuse is the same as that of the fresh catalyst as estimated by ICP-AES. TEM images of the reused catalyst showed an almost similar morphology to that of the fresh catalyst (Fig. S3 in the ESI†). The retention of the Mn-HTS structure was further confirmed by comparison of the XRD (Fig. S1 in the ESI†), FT-IR (Fig. S4 in the ESI†) and UV-Vis (Fig. 4A) spectra of the fresh and the 15 times reused catalyst. These results support the behavior of Mn-HTS as a truly heterogeneous catalyst during cyclohexanone oxidation, which proves the efficacy of the catalyst in industry.

3.5 The formation route of AA from cyclohexanone

An important issue then arose: the formation route of AA from cyclohexanone. Generally, cyclic ketones tend to form corresponding diacids with molecular oxygen *via* a radical autoxidation mechanism or a redox-type mechanism.[34] The simultaneous C–C and O–O cleavage in the metal cyclohexylperoxo complex seemed to be the breakthrough point to form AA *via* a redox-type pathway.[37] If this hypothesis was right, the complex should be easily converted to 6-hydroxyhexanoic acid under the same conditions. Unexpectedly, no 6-hydroxyhexanoic acid was detected by GC-MS. Furthermore when a small amount of a radical inhibitor (5 mol% 2,6-di-*tert*-butyl-*p*-cresol) was added, cyclohexanone conversion was nil (Table 1,

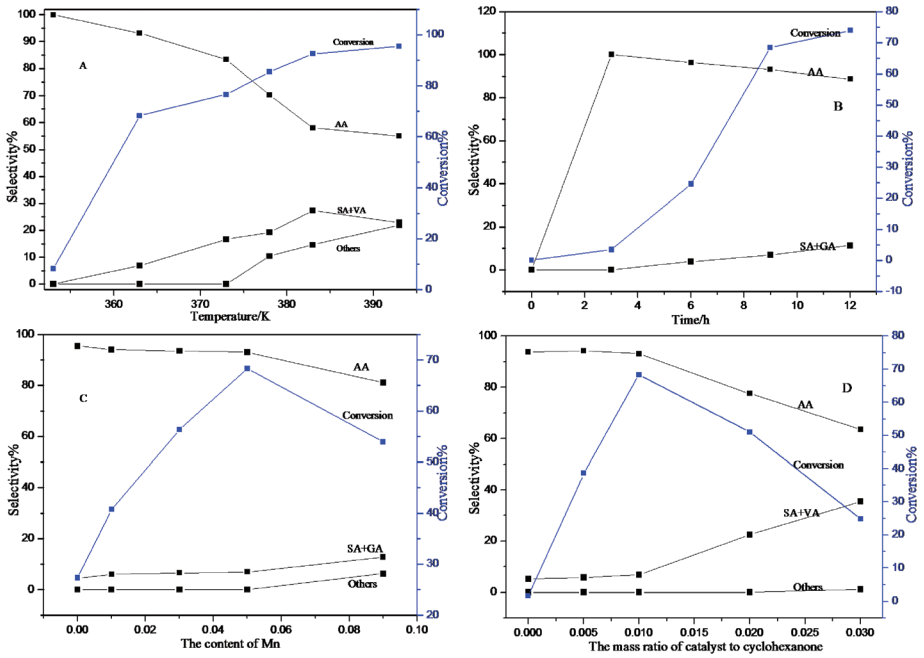

Fig. 6 Effect of the reaction temperature (A), reaction time (B), Mn loading amount (C) and catalyst amount (D) on the conversion of cyclohexanone and AA selectivity over the synthesized 5% Mn-HTS (reaction conditions: 40 g cyclohexanone; GA + SA: glutarate acid and succinate acid; others include CO_2 and CO).

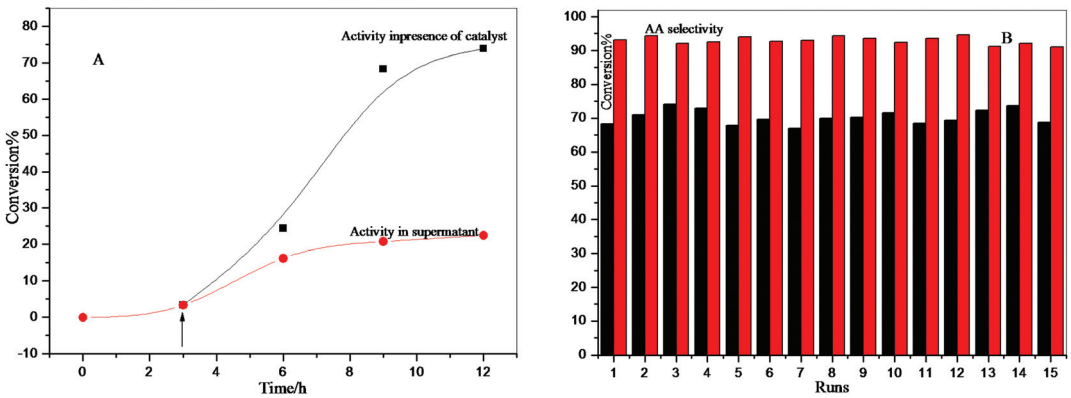

Fig. 7 Results of hot-separation (A) and recycle (B) test of the 5% Mn-HTS catalyst at 363 K (reaction conditions: 0.6 MPa O_2, cyclohexanone 40 g, catalyst 0.4 g).

entry 16), suggesting that the main reaction course might be a free-radical one. From the effects of reaction parameters, no lighter diacids derived from 2-hydroxylcyclohexanone were detected at first (1–3 h). All these results above indicated that the Mn-HTS catalyzed oxidation of cyclohexanone was quite different from those using a Co/Mn cluster, $H_5PMo_{10}V_2O_{40}$, $H_7PMo_8V_4O_{40}$ or $Mn(OAc)_2$-based catalytic systems.[9,38–40] In those examples, AA was often generated *via* a redox-type reaction with electron transfer from the substrate to the catalyst, as proposed by the authors.

In contrast, the use of acetic acid as the additive greatly enhanced the reaction rate, as shown in Table 1 (entry 14). An explanation is the *in situ* formation of CH_3COOOH, which might eventually act as an oxidant on cyclohexanone oxidation; however, separate tests of acetic acid oxidation with oxygen and the Mn-HTS catalyst led us to exclude the formation of any peracid, as inferred by iodometric titration. A similar acceleration effect, although has been already reported in the aerial cyclohexanone or cyclohexane using Mn and Mn/Co catalysts in the past decade, have almost never been considered.[41,42] Based on the different configurational isomers of the reactant cyclohexanone, in this work we have imagined two possible isomers: keto-form and enol-form. The optimized structures of the cyclohexanone isomers were investigated by the DFT method with the B3LYP correlation functional and are shown in Fig. 8. Calculation results indicate that in both the isomers, one of the C–H bonds [C(2)–H(7)] connecting the carbonyl or hydroxyl group is longer than [C(1)–H(9)] near the methylene

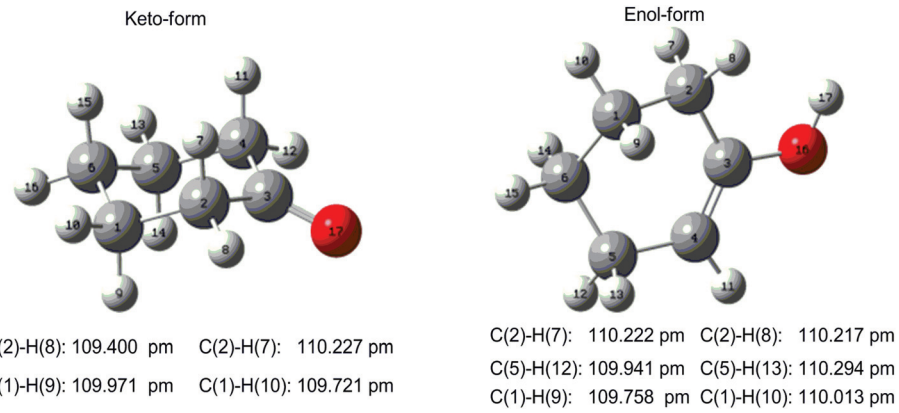

Fig. 8 Calculated bond lengths of cyclohexanone including keto-form and enol-form.

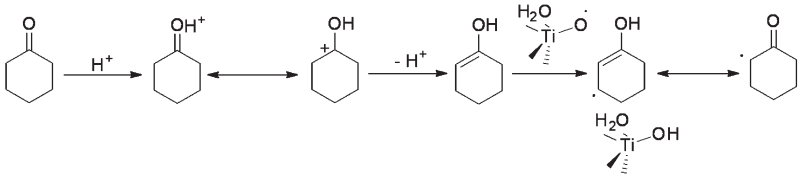

Scheme 1 The activation of cyclohexanone *via* protonation and tautomerisation.

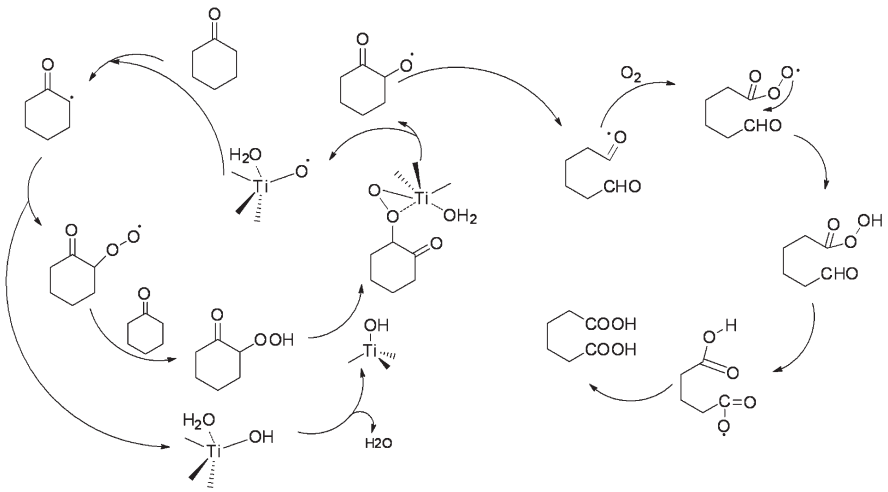

Scheme 2 Proposed mechanism for the Mn-HTS catalyzed formation of AA.

group; thus it is easily broken from C(2)–H(7) to produce a radical. From a different standpoint, the carbon–hydrogen bond [C(5)–H(13) or C(2)–H(7)] of the enol-form connects a double bond and the corresponding bond distance [C(5)–H(13)] is larger than that of the [C(2)–H(7)] bond. As a result, it was more easy for homolytic cleavage of the longer [C(5)–H(13)] bond to produce the radical for enol-form isomers. Therefore, a possible explanation for this effect is the acceleration of the tautomerism between cyclohexanone and the corresponding enolic form by the addition of acetic acid, which is more easily activated by radical H abstraction than cyclohexanone itself to produce radical species (Scheme 1). The use of AA as the additive instead of acetic acid also shows outstanding effects in the acceleration of the reaction rate, which confirms the acceleration of the tautomerism between cyclohexanone and the corresponding enolic form under acidic conditions. It is evident that the oxidation occurs easily upon the Mn-modified HTS. According to the pyridine-adsorbed FT-IR spectra results, Mn-HTS catalysts possess more acid sites, which favor the formation of enolate from the keto-form of cyclohexanone in the oxidation process. Based on the experiments and DFT theoretical calculation mentioned above,

we have proposed a pathway for Mn-HTS catalyzed oxidation of cyclohexanone with molecular oxygen (Scheme 2). The H-abstraction at the carbon adjacent to the oxygen in cyclohexanone (or adjacent to a double bond in enol-form isomers by tautomerism) can most likely be promoted in the presence of Ti species, and the production of radical at this position readily leads to the formation of cyclohexyl hydroperoxide with oxygen. This product is prone to be captured by Ti–OH species to produce Ti(OOCh) species, which can be decomposed into active Ti(IV)–O species and a ketonyl radical.[43–45] The ketonyl radical then reacts to yield the radical species OHC–$(CH_2)_4$–C(O) by the ring opening *via* C–C scission; successive oxidation steps lead to the formation of AA.[34] In this oxidation reaction, Mn species performs a dual role, promoting the production of radical intermediates to increase the reaction rate and also the tautomerism between cyclohexanone and the corresponding enolic form.

4. Conclusion

To summarize, the hollow-structured Mn-HTS demonstrates superior catalytic activity and selectivity in the oxidation of cyclohexanone to adipic acid with O_2 under mild solvent-free and promoter-free conditions. The data in Table S1 in the ESI,† compare the results obtained over hollow-structured Mn-HTS and other catalytic systems used for this reaction. This new HTS catalytic material behaving as a true heterogeneous catalyst can be recycled and reused in several catalytic iterations without losing its catalytic activity. This opens great perspectives in terms of catalytic industrial processes and sheds light on developing strategies aimed at rendering titanosilicate molecular sieves with new functionalities. Moreover, an innovative approach to produce AA avoids the nitric oxidation route which generates a strong greenhouse gas, and thus provides an environmentally benign alternative for an important industrial reaction.

Notes and references

1 G.-J. Brink, I. W. C. E. Arends and R. A. Sheldon, *Science*, 2000, **287**, 1636–1639.
2 D. D. Davis and D. R. Kemp, in *Kirk–Othmer Encyclopedia of Chemical Technology*, ed. J. I. Kroscwitz and M. Howe-Grant, John Wiley & Sons, Inc., New York, 4th edn, 1991, vol. 1, pp. 466–493.
3 J. M. Thomas and R. Raja, *Chem. Commun.*, 2001, 675–687.
4 F. Cavani and S. Alini, in *Sustainable Industrial Chemistry*, ed. F. Cavani, G. Centi, S. Perathoner and F. Trifirò, Wiley-VCH, Weinheim, 2009, pp. 367–425.
5 A. Castellan, J. C. J. Bart and S. Cavallaro, *Catal. Today*, 1991, **9**, 237–254.
6 U. Schuchardt, D. Cardoso, R. Sercheli, R. Pereira, R. S. da Cruz, M. C. Guerreiro, D. Mandelli, E. V. Spinacé and E. L. Pires, *Appl. Catal., A*, 2001, **211**, 1–17.
7 S. A. Montzka, E. J. Dlugokencky and J. H. Butler, *Nature*, 2011, **476**, 43–50.
8 S. Ghosh, S. S. Acharyya, S. Adak, L. N. S. Konathala, T. Sasakib and R. Bal, *Green Chem.*, 2014, **16**, 2826–2834.
9 S. A. Chavan, D. Srinivas and P. Ratnasamy, *J. Catal.*, 2002, **212**, 39–45.
10 Y. Usui and K. Sato, *Green Chem.*, 2003, **5**, 373–375.
11 Z. Bohström and I. R.-L. K. Holmberg, *Green Chem.*, 2010, **12**, 1861–1869.
12 R. Raja, G. Sankar and J. M. Thomas, *J. Am. Chem. Soc.*, 1999, **121**, 11926–11927.
13 P. Ratnasamy, D. Srinivas and H. Knözinger, *Adv. Catal.*, 2004, **48**, 1–169.
14 A. Corma, M. A. Camblor, P. Esteve, A. Martínez and J. Pérez-Pariente, *J. Catal.*, 1994, **145**, 151–158.
15 E. V. Spinace, H. O. Pastore and U. Schuchardt, *J. Catal.*, 1995, **157**, 631–635.
16 Y. Goa, P. Wu and T. Tatsumi, *J. Phys. Chem. B*, 2004, **108**, 8401–8411.
17 M. Reichinger, W. Schmidt, M. W. E. van den Berg, A. Aerts, J. A. Martens, C. E. A. Kirschhock, H. Gies and W. Grünert, *J. Catal.*, 2010, **269**, 367–375.
18 M. Moliner, P. Serna, Á. Cantin, G. Sastre, M. J. Díaz-Cabanas and A. Corma, *J. Phys. Chem. C*, 2008, **112**, 19547–19554.
19 B. P. C. Hereijgers and B. M. Weckhuysen, *J. Catal.*, 2010, **270**, 16–25.
20 W. Fan, P. Wu, S. Namba and T. Tatsumi, *J. Catal.*, 2006, **243**, 183–191.
21 C. Shi, B. Zhu, M. Lin, J. Long and R. Wang, *Catal. Today*, 2011, **175**, 398–403.
22 G. Zou, W. Zhong, Q. Xu, J. Xiao, C. Liu, Y. Li, L. Mao, S. Kirk and D. Yin, *Catal. Commun.*, 2015, **58**, 46–52.
23 Y. Wang, M. Lin and A. Tuel, *Microporous Mesoporous Mater.*, 2007, **102**, 80–85.
24 W.-S. Lee, M. C. Akatay, E. A. Stach, F. H. Ribeiro and W. N. Delgass, *J. Catal.*, 2012, **287**, 178–189.
25 J. C. Groen, T. Bach, U. Ziese, A. M. P. Donk, K. P. D. Jong, J. A. Moulijn and J. P. Pe′rez-Ramirez, *J. Am. Chem. Soc.*, 2005, **127**, 10792–10793.
26 G. Ricchiardi, A. Damin, S. Bordiga, C. Lamberti, G. Spano, F. Rivetti and A. Zecchina, *J. Am. Chem. Soc.*, 2001, **123**, 11409–11419.
27 L. Wang, Y. Liu, W. Xie, H. Wu, X. Li, M. Y. He and P. Wu, *J. Phys. Chem. C*, 2008, **112**, 6132–6138.
28 M. Baldi, F. Milella and J. M. Gallardo-Amores, *J. Mater. Chem.*, 1998, **8**, 2525–2531.
29 M. Kang and M.-H. Lee, *Appl. Catal., A*, 2005, **284**, 215–222.
30 Y. Xu, B. Lei, L. Guo, W. Zhou and Y. Liu, *J. Hazard. Mater.*, 2008, **160**, 78–82.
31 P. Dhage, A. Samokhvalov, D. Repala, E. C. Duin and B. J. Tatarchuk, *Phys. Chem. Chem. Phys.*, 2011, **13**, 2179–2187.
32 C.A. Emeis, *J. Catal.*, 1993, **141**, 323–743.
33 T. Punniyamurthy, S. Velusamy and J. Iqbal, *Chem. Rev.*, 2005, **105**, 2329–2363.

34 F. Cavani, L. Ferroni, A. Frattini, C. Lucarelli, A. Mazzini, K. Raabova, S. Alini, P. Accorinti and P. Babini, *Appl. Catal., A*, 2011, **391**, 118–124.
35 I. Belkhir, A. Germain, F. Fajula and E. Fache, *J. Chem. Soc., Faraday Trans.*, 1998, **94**, 1761–1764.
36 E. Breynaert, I. Hermans, B. Lambie, G. Maes, J. Peeters, A. Maes and P. A. Jacobs, *Angew. Chem., Int. Ed.*, 2006, **45**, 7584–7588.
37 M. Vennat, P. Herson, J.-M. Brégeault and G.B. Shul'pin, *Eur. J. Inorg. Chem.*, 2003, 908–917.
38 J. M. Brégeault, E. A. Bassam and J. Martin, *US Patent* 4983767, 1991 (patent held by Rhone Poulenc Chimie).
39 A. Atlamsani, J.-M. Brégeault and M. Ziyad, *J. Org. Chem.*, 1993, **58**, 5663–5665.
40 M. Constantini and L. Krumenacker, *FR Patent* 2541993, 1983 (patent held by Rhone Poulenc).
41 A. Shimizu, K. Tanaka, H. Ogawa, Y. Matsuoka, M. Fujimori, Y. Nagamori, H. Hamachi and K. Kimura, *Bull. Chem. Soc. Jpn.*, 2003, **76**, 1993–2001.
42 D. Bonnet, T. Ireland, E. Fache and J.-P. Simonato, *Green Chem.*, 2006, **8**, 556–559.
43 J. Zhuang, G. Yang, D. Ma, X. Lan, X. Liu, X. Han, X. Bao and U. Mueller, *Angew. Chem., Int. Ed.*, 2004, **43**, 6377–6381.
44 D. Srinivas, P. Manikandan, S. C. Laha, R. Kumar and P. Ratnasamy, *J. Catal.*, 2003, **217**, 160–171.
45 G. Clerici, *Top. Catal.*, 2001, **15**, 257–263.